NANO LETTERS

pubs.acs.org/NanoLett Letter

Phosphatidylserine Lipid Nanoparticles Promote Systemic RNA Delivery to Secondary Lymphoid Organs

Sijin Luozhong,[#] Zhefan Yuan,[#] Tara Sarmiento, Yu Chen, Wenchao Gu, Caleb McCurdy, Wenting Gao, Ruoxin Li, Stephan Wilkens, and Shaoyi Jiang*

Cite This: *Nano Lett.* 2022, 22, 8304−8311 Read Online

ACCESS | Metrics & More | Article Recommendations | Supporting Information

ABSTRACT: Secondary lymphoid organs (SLOs) are an important target for mRNA delivery in various applications. While the current delivery method relies on the drainage of nanoparticles to lymph nodes by intramuscular (IM) or subcutaneous (SC) injections, an efficient mRNA delivery carrier for SLOs-targeting delivery by systemic administration (IV) is highly desirable but yet to be available. In this study, we developed an efficient SLOs-targeting carrier using phosphatidylserine (PS), a well-known signaling molecule that promotes the endocytic activity of phagocytes and cellular entry of enveloped viruses. We adopted these biomimetic strategies and added PS into the standard four-component MC3-based LNP formulation (PS-LNP) to facilitate the cellular uptake of immune cells beyond the charge-driven targeting principle commonly used today. As a result, PS-LNP performed efficient protein expression in both lymph nodes and the spleen after IV administration. *In vitro* and *in vivo* characterizations on PS-LNP demonstrated a monocyte/macrophage-mediated SLOs-targeting delivery mechanism.

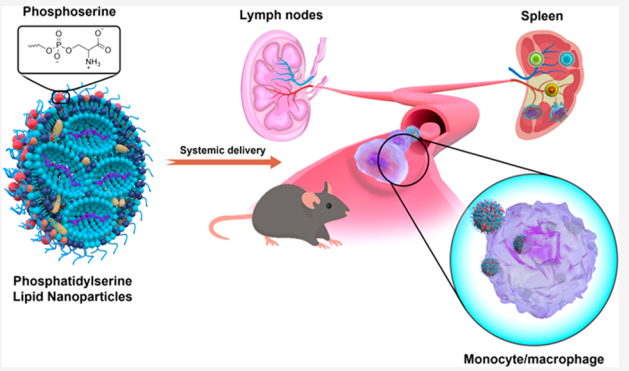

KEYWORDS: *lipid nanoparticles, mRNA delivery, secondary lymphoid organs, cell-targeting delivery*

Lipid nanoparticles (LNPs) have successfully enabled the clinical applications of mRNA (mRNA) therapeutics, particularly their remarkable success in COVID-19 vaccines.[1] LNPs protect mRNA from nuclease degradation and rapid clearance from blood circulation and facilitate cellular uptake.[2] A typical LNP formulation is made up of ionizable cationic lipids, helper lipids, cholesterol, and polyethylene glycol (PEG)-lipids. To date, most reported LNP formulations tend to accumulate in the liver among all organs upon systemic administration.[3] For example, the first FDA-approved LNP drug, based on DLin-MC3-DMA (MC3) as ionizable lipids, was shown to be predominantly expressed by the liver.[4,5] LNPs based on other ionizable lipids were also shown strong protein expression of mRNA in the liver, including C12−200,[6] cKK-E12,[7] and SM-102.[8] While these formulations offer the feasibility of mRNA therapy for liver diseases, nonhepatic delivery of LNPs is still challenging due to the intrinsic liver tropism of nanoparticles.[9−11]

Efficient mRNA delivery to secondary lymphoid organs (SLOs) by systemic administration is highly needed. SLOs, including lymph nodes (LNs) and the spleen, are pivotal environments where immune cells interact with one another to initiate adaptive immunity.[12] The introduction of functional mRNA to these cells enables applications including immunotherapy against cancer or autoimmune diseases, and gene editing for cell engineering. Up to date, most approaches to delivering mRNA-based vaccines have relied on LN drainage via IM or SC injections.[12] Upon injections, immune cells, such as neutrophils and monocytes, are recruited to the site of injections, take up the particles and then mobilize to the draining LNs to perform T cell priming. However, many cells that internalize LNPs cannot efficiently express proteins from mRNA, particularly neutrophils.[13] Moreover, nonimmune cells at the injection site, including epithelial cells and muscle cells, also take up most of the injected LNP but do not participate in antigen presentation occurring in draining LNs.[11] In either case, the delivery efficiency of mRNA is suboptimal. Thus, a more potent delivery strategy is needed to target immune cells in SLOs. Alternatively, IV delivery of mRNA has the advantage over IM or SC delivery to access most LNs in the body via the bloodstream and spleen where most immune cells locate. However, it is hindered by the risk of off-target effects that cause potential systemic toxicity. Several studies attempted to

Received: August 15, 2022
Revised: September 26, 2022
Published: October 4, 2022

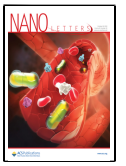

https://doi.org/10.1021/acs.nanolett.2c03234
Nano Lett. 2022, 22, 8304−8311

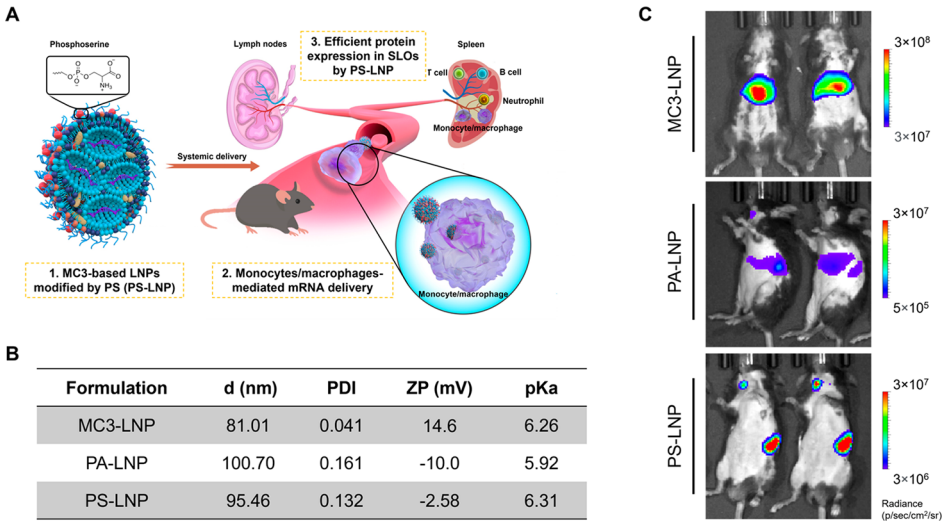

B

Formulation	d (nm)	PDI	ZP (mV)	pKa
MC3-LNP	81.01	0.041	14.6	6.26
PA-LNP	100.70	0.161	-10.0	5.92
PS-LNP	95.46	0.132	-2.58	6.31

Figure 1. Illustrations and characterization of phosphatidylserine-containing lipid nanoparticles (PS-LNP) targeted deliver mRNA to SLOs. (A) The targeted delivery of PS-LNP to the spleen and lymph node (or SLOs) was mediated by "monocytes/macrophages": (1) PS-LNP is formulated by an MC3-based LNP modified by PS for targeting SLOs; (2) Monocytes/macrophages mediate the SLOs-targeting delivery of PS-LNP; (3) PS-LNP delivers mRNA to lymph nodes and the spleen and induces efficient protein expression. (B) Conventional MC3-based four-component LNPs (MC3-LNP), LNPs with 18PA (PA-LNP), and with DOPS (PS-LNP) were formulated to encapsulate mRNA encoding firefly's luciferase (Fluc), and characterized, respectively. (C) All LNPs encapsulating Fluc-mRNA (0.2 mg/kg) were injected into C57BL/6J by retro-orbital injections. Whole-body IVIS images were performed at 6 h after administration. Both inclusions of PA and PS into the MC3-based formulations shifted the biodistribution of protein expression from the liver to the spleen. However, PS-LNP showed higher efficiency in the spleen and also potent expression in superficial cervical lymph nodes (SCLNs). Note that the lower limit of the color scale bar of PS-LNP is an order of magnitude higher than that of PA-LNP.

achieve spleen-targeting delivery of mRNA, either actively or passively by manipulating the properties of LNPs.[14] For active targeting, LNPs are usually coated with targeting antibodies or surface ligands to utilize interaction with receptors on the surface of the target cell.[15,16] Although conjugating antibodies can be a straightforward method, the stability of LNPs may be compromised. Furthermore, the selection of a targeting moiety is greatly limited by the generation of corresponding antibodies.[16] On the other hand, passive targeting, which does not rely on targeting moieties, manipulates the architecture of the particle, such as charge and size. For example, Kranz et.al adjusted the ratio between mRNA and cationic lipids of the mRNA-lipoplex formulation to vary the negative net charge of the nanoparticle. While the negatively charged nanoparticle preferentially delivered mRNA to the spleen, the transfection efficiency declined as the negative charge of the nanoparticles increased. Nevertheless, this study is an excellent example that demonstrates the practicability of the systemic delivery of mRNA in cancer immunotherapy.[17] In another study, Cheng et.al incorporated an anionic lipid, 1,2-dioleoyl-*sn*-glycero-3-phosphate (18PA), into the liver-targeting LNP formulations and was able to deliver the mRNA to the spleen following IV administration.[18] The altered biodistribution was a consequence of the extra negative charge which changes the composition of corona proteins on LNPs.[19] Similarly, increasing the amount of anionic components in the formulation led to a higher accumulation of mRNA in the spleen but a reduced protein expression from mRNA.[17,18]

In this work, we sought to achieve efficient SLOs-targeting mRNA delivery in a biomimetic manner. To this end, we modified the LNP system to actively enhance the uptake of LNPs by certain cell types in SLOs. In nature, phosphatidylserine (PS) is a well-characterized membrane molecule that is recognized by phagocytes, such as macrophages, and increases their endocytic activity. Externalization of PS in apoptotic cells sends a signal to phagocytes for endocytic engulfment.[20] Furthermore, many enveloped viruses exploit a similar mechanism to promote their cellular entry and thus infection efficiency. These viruses hijack the PS components from the endothelium reticulum or cell membrane and incorporate them into their viral membrane during the budding process, so they can bind to the corresponding receptors on the host cells and facilitate infection.[21] Therefore, we added 1,2-dioleoyl-*sn*-glycero-3-phospho-L-serine (DOPS) into the standard four-component MC3-based formulation (MC3-LNP) containing MC3, 1,2-distearoyl-*sn*-glycero-3-phosphocholine (DSPC), cholesterol and 1,2-dimyristoyl-rac-glycero-3-methoxypolyethylene glycol-2000 (DMG-PEG2000) to form a SLO-targeting formulation (PS-LNP) (Figure 1A). Meanwhile, another anionic lipid without the functional phosphoserine group for active targeting, 18PA, was also used to generate LNPs (PA-LNP) as a reference to compare with PS-LNP (Figure S1 and Figure S2).[18] First, dynamic light scattering confirmed the encapsulation and size of LNPs for MC3-, PA- and PS-LNP, respectively (Figure 1B and Figure S3). Zeta-potential measurements of the particles demonstrated that MC3-LNP was slightly positively charged, while PS- and PA-LNP were negatively charged (Figure 1B). The encapsulation efficiency of all the formulations was shown to be >85%. All formulations were tested to have a similar pK_a value: MC3-LNP (pK_a = 6.26), PA-LNP (pK_a = 5.92), and PS-LNP (pK_a = 6.31) (Figure S3). Cryogenic transmission electron microscopy (Cryo-EM) images were taken to show the morphology of each LNP formulation, respectively (Figure S4).

First, we evaluated the location of Fluc expression in C57BL/6J mice after IV injection of the above LNPs. In this study, IVIS imaging on the whole body was conducted at 6 h

https://doi.org/10.1021/acs.nanolett.2c03234
Nano Lett. 2022, 22, 8304−8311

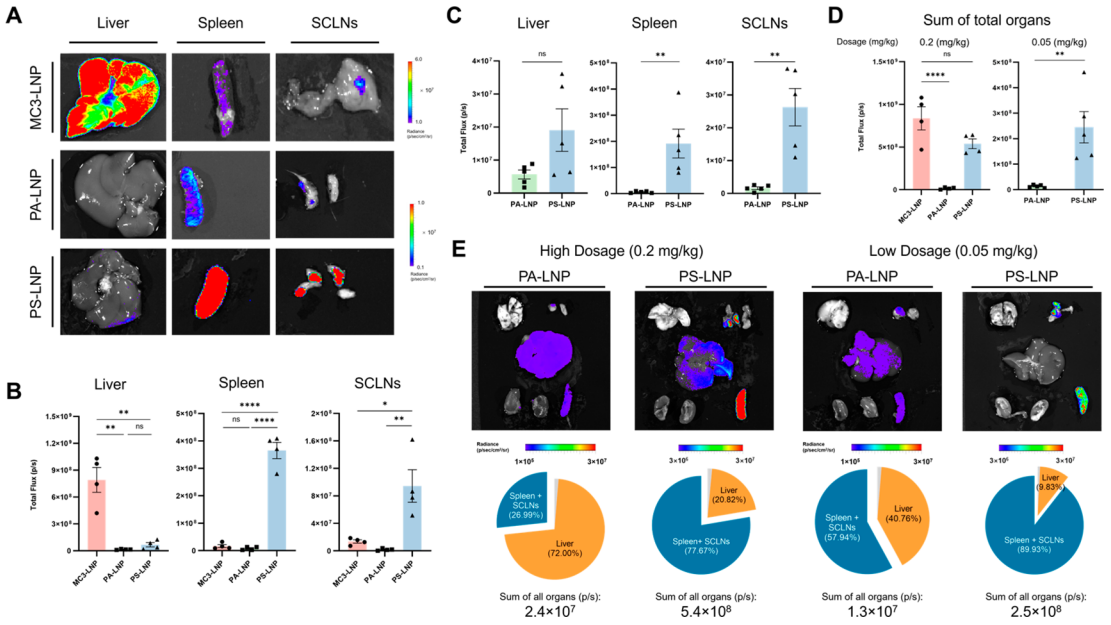

Figure 2. Biodistribution of Fluc expression after intravenous injections of different LNPs encapsulating Fluc mRNA. (A,B) At a dosage of 0.2 mg/kg (high dosage), IVIS images were taken on isolated organs (A), and the bioluminescence signal was analyzed to get total luminescence flux in the liver, the spleen, and superficial cervical lymph nodes (SCLNs, attached on the adjacent fat) (B). As a result, MC3-LNP had most of the expression in the liver but less in the spleen and SCLNs. In contrast, PS-LNP showed potent expression in the spleen and SCLNs. Although PA-LNP had a shifted distribution from the liver to the spleen, the luminescence activity was significantly weaker than that of PS-LNP ($p < 0.0001$) but similar to that of MC3-LNP ($p = 0.21$). Luminescence signal in the spleen (PS-LNP, 3.7×10^8; PA-LNP, 8.0×10^6; MC3-LNP, 1.7×10^7; total flux (p/s)). In SCLNs, only PS-LNP showed potent Fluc expression (PS-LNP, 9.4×10^7; PA-LNP, 1.8×10^6; MC3-LNP, 1.4×10^7; total flux (p/s). (C) At a dosage of 0.05 mg/kg (low dosage), the expression level in different organs was compared between PA- and PS-LNP. While PS- had a similar liver expression as PA-LNP ($p = 0.07$), significantly higher expression levels were found in the spleen and SCLNs from the PS-LNP. (D) The sum of all luminescence signals from all organs was shown at high dosage (left) and low dosage (right). The result indicates that the addition of phosphatidylserine confers SLOs targeting effect without compromising the transfection efficiency. (E) Comparison of the performance of targeted delivery to SLOs between PA and PS-LNP at high dosage and low dosage, respectively. The relative expression in each organ was analyzed by calculating the percentage of the total luminescence flux of all organs. As a result, at low dosage, PS-LNP had potent targeted mRNA delivery to the spleen and SCLNs with a ~90% relative expression level among other organs. However, the targeting effect was weaker in PA-LNP, where ~40% of the luminescence signal was still present in the liver and only 60% in the spleen and SCLNs. Although the percentage of liver expression from PS-LNP started to increase at high dosage, SLOs targeting effect was still maintained at a high level (~78%) and more effective than that from PA-LNP (~27%). The signal in the lung and kidneys was detected to be negligible for all groups. Organs shown here are (from top to bottom) lung, SCLNs (attached to the fat), liver, kidneys, and spleen. Images were analyzed using Living Image software (PerkinElmer). A two-tailed t test was conducted to analyze the statistical difference. (* $p < 0.05$; ** $p < 0.01$; *** $p < 0.001$; **** $p < 0.0001$). Biological replicates of the experiment ($n = 4$ or 5) were indicated as scatters in the plot. Data are shown as mean ± SEM.

after administration at a high dosage (0.2 mg/kg). As reported before, MC3-LNP showed maximal protein expression in the liver.[5] Both PA- and PS-LNP showed a shift of luciferase expression from the liver to the spleen, but the luminescent signal was much stronger in the PS-LNP (Figure 1C). Furthermore, we discovered that PS-LNP had a significant increase in luciferase expression in superficial cervical lymph nodes (SCLNs) which was not detected in either MC3- or PA-LNP. The distribution patterns of these three formulations are consistent at 24 and 48 h after administration (Figure S5 and Figure S6). To compare the expression level more accurately, we analyzed the bioluminescence signal on isolated organs at 6 h after administration of LNPs (Figure 2A). As a result, the Fluc expression from MC3-LNP predominantly occurred in the liver and less in the spleen. In contrast, adding PS to the formulation drastically reduced the Fluc expression in the liver and had most of the expression in the spleen. PA-LNP also had reduced Fluc expression in the liver, but the expression in the spleen was 45-fold weaker than that of PS-LNP. Expression in the spleen of PA-LNP was not statistically different from that of MC3-LNP ($p = 0.21$). (Figure 2B) More importantly, we observed potent Fluc expression in SCLNs from PS-LNP but little from other groups (Figure 2B). We further compared the targeting effect of PA- and PS-LNP at a lower dosage (0.05 mg/kg) (Figure 2C and Figure S7). In the spleen and SCLNs, the luminescence signal was stronger in PS-LNP than in PA-LNP by an order of magnitude (Figure 2C). Therefore, the results demonstrated an efficient biodistribution shift toward SLOs after adding PS into the MC3-LNP formulation. Notably, the addition of PS promotes the targeting of mRNA LNPs to the spleen and SCLNs far more efficiently than that of PA-LNP. The total luminescence signal produced by all organs was significantly higher in PS-LNP than in PA-LNP at either dosage. Also, the signal was at the same level in both MC3- and PS-LNP at a dosage of 0.2 mg/kg ($p = 0.09$) (Figure 2D). The result implies that, unlike PA-LNP, PS-LNP achieved targeted expression while maintaining a high transfection efficiency. Furthermore, we analyzed the relative expression in each organ by calculating the percentage of the total luminescence flux (Figure 2E). At the lower dosage, we found that PS-LNP completely altered delivery to the spleen and SCLNs (~90%) from the liver (~10%), whereas the targeting effect was much weaker in PA-LNP with ~41% in the liver and only ~58% in the spleen and SCLNs. When the

https://doi.org/10.1021/acs.nanolett.2c03234
Nano Lett. 2022, 22, 8304−8311

dosage was increased to 0.2 mg/kg, the percentage of expression in the spleen and SCLNs slightly reduced to ~78%. A possible explanation for the reduction is that the capacity of protein expression in the liver is larger than in the spleen. Nonetheless, the SLOs-targeting effect of PS-LNP was still more prominent than that of PA-LNP (~27%). The reported PA-LNP formulation used an excessive amount of anionic lipids (18 PA) to achieve effective spleen targeting, which makes low transfection efficiency anticipated because it is unfavorable for overcoming the barrier of the anionic cell membrane.[22] Therefore, the PS-LNP formulation utilizing a small amount of targeting lipid (PS) is preferred to achieve the efficient targeted delivery of mRNA to the spleen and SCLNs.

Next, we investigated the biodistribution of LNPs by imaging isolated organs in the IVIS at 4 h after systemic injection of LNPs encapsulating a Cy5-labeled RNA (Figure 3A). First, we examined the Cy5 signal present in the main lymph nodes, including superficial cervical, axillary, brachial, and inguinal lymph nodes. Contrary to MC3- and PA-LNP in which fluorescent signal was barely seen, all lymph nodes in PS-LNP showed Cy5 signal at different levels with SCLNs being the strongest one (Figure 3A and Figure S8A). A negligible amount of fluorescent signal was detected in LNs extracted from mice treated with PBS or Cy5-RNA alone (Figure 3A and Figure S8B). The total radiance efficiency was quantified to indicate the amount of Cy5-RNA taken up by the cells in the LNs (Figure 3B). As a result, PS-LNP demonstrated the strongest fluorescent signal among other groups. Furthermore, more than 90% of the signal was produced from SCLNs. The result could be explained by the fact that SCLNs are the closest lymph nodes from where the drug was administered (ophthalmic venous sinus). Then, we analyzed the Cy5 signal in the liver and spleen (Figure 3B). No prominent difference in Cy5 epifluorescence signal was found in both the liver and spleen among all groups. However, it is worth noting that the liver and spleen are two main organs where most LNPs accumulate after systemic delivery.[23,24] Hence, PA- as well as PS-LNP did not alter the biodistribution of the particle in both the liver and spleen as in the case of MC3-LNP. PS-LNP achieved targeted delivery of mRNA by performing selective high transfection in the spleen. PS-LNP had much higher expression in the spleen, indicating its targeting effect without sacrificing the transfection efficiency. Following a charge-driven design principle, LoPresti et al. introduced negatively charged PS lipids into their LNP systems and compared organ-specific expression in the liver, spleen, and lungs.[25] In this work, however, we proposed a biomimetic design principle of PS recognition by phagocytes and evaluated the biodistribution of LNPs in secondary lymphoid organs, including the spleen and systemic lymph nodes. The high fluorescent signal in LNs from PS-LNP indicates the active transportation of LNPs after systemic delivery, not simply due to the charge effects, which was not observed before. Overall, our results suggested an active mechanism via a biomimetic functional group, leading to enhanced cellular uptake of PS-LNP in the spleen and lymph nodes.

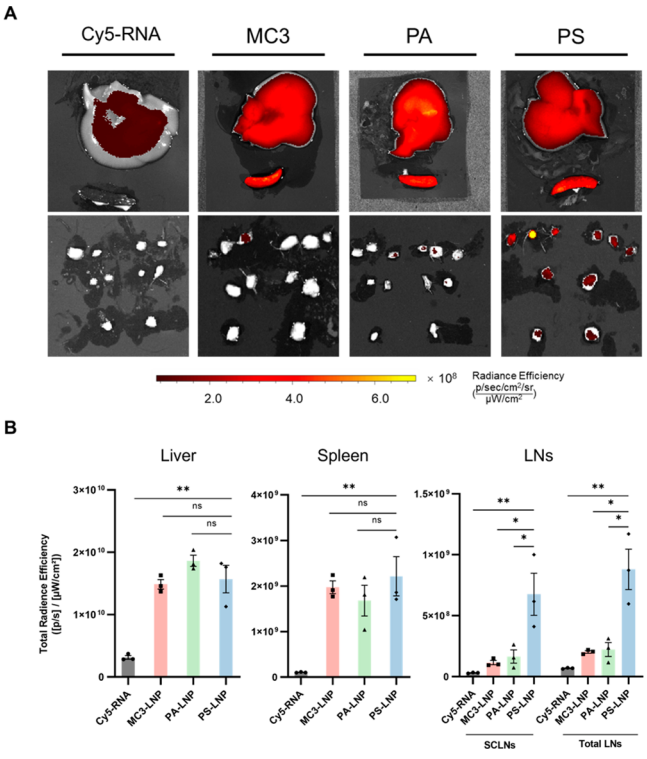

Figure 3. Evaluation of the biodistribution of the particle by Cy5 labeled-mRNA. LNPs encapsulating Cy5 labeled-mRNA were injected systemically into C57BL/6J mice (0.5 mg/kg). The same amount of Cy5-labeled RNA without LNPs was injected as a control. (A) Fluorescent images were taken on isolated organs to show Cy5 signal in the liver and the spleen (upper row), and lymph nodes (lower row). Major lymph nodes from the mouse were isolated, including superficial cervical lymph nodes (SCLNs), axillary LNs, brachial LNs, and inguinal LNs from both sides of the body, respectively. (B) Quantification of epifluorescence on lymph nodes, the liver, and the spleen. No significant difference was found in Cy5 signal from the liver and the spleen among all groups. However, PS-LNP was able to transport mRNA to LNs, especially to the SCLNs. Images were analyzed using Living Image software (PerkinElmer). A two-tailed *t* test was conducted to analyze the statistical difference. (* $p < 0.05$; ** $p < 0.01$;). Biological replicates of the experiment ($n = 3$) were indicated as scatters in the plot. Data are shown as mean ± SEM.

Having confirmed SLOs-targeting delivery of PS-LNP by both particle biodistribution and protein expression, we sought to understand the active mechanism behind the targeted protein expression. In nature, the phosphoserine functional group can be found on a natural lipid PS, which serves as an "eat-me" signal to phagocytes by binding to the scavenger receptors on the cell surface.[26,27] We hypothesized that the addition of phosphatidylserine facilitates the accumulation of LNPs in SLOs, a process resembling the natural mechanism where PS promotes the clearance of apoptotic cells by phagocytes.[20] First, we conducted an in vitro luciferase assay to compare the transfection efficiency of MC3- and PS-LNP in HepG2, a hepatocyte cell line, and RAW264.7, a monocyte/macrophage cell line, respectively (Figure S9). As a result, MC3-LNP demonstrated around 10 times the expression level higher than PS-LNP in HepG2, whereas PS-LNP performed better in transfection of RAW264.7. Similar to the result in immortal cell lines, PS-LNP had a higher transfection efficiency in primary murine splenocytes than MC3-LNP. Therefore, the incorporation of PS lipids into the LNP formulation increases the mRNA transfection in immune cells, especially macrophages. These results explained why particle distribution does not necessarily correlate with protein expression in mRNA delivery. Although most of the particles accumulate in the liver (as shown in Figure 3A), PS-LNP induced weak protein expression in the liver (as shown in Figure 2A). On the

https://doi.org/10.1021/acs.nanolett.2c03234
Nano Lett. 2022, 22, 8304−8311

contrary, PS-LNP outperformed in transfecting macrophages and splenocytes, resulting in a selective protein expression in SLOs.

The in vitro transfection data prompted us to question if certain types of immune cells, such as macrophages, play a critical role in the SLO-targeting delivery of PS-LNP. We then studied which cell types from the spleen take up the particle through flow cytometry analysis. Briefly, C57BL/6J mice were given MC3- or PS- LNP encapsulating Cy5-labeled mRNA via IV injections. After 4 h, single cells were extracted from the spleen and analyzed for $Cy5^+$ cells by flow cytometry (Figure S10 and Figure S11).[28,29] As a result, a larger $CD45^+$ population was found to be $Cy5^+$ in PS-LNP (~1.05%) than MC3-LNP (~0.24%) (Figure 4A). A breakdown of $CD45^+Cy5^+$ populations from PS-LNP treated mice shows that over 50% of cells are myeloid cells (Figure 4B). First, we analyzed Cy5-RNA uptake by monocytes/macrophages using two gating strategies, including F4/80-based and Ly6G/Ly6C-based strategies.[28] As shown in Figure 4C, the percentage of $Cy5^+$ monocytes/macrophages was over 2-fold higher in PS-LNP than in MC3-LNP. The increased percentage indicates an enhanced uptake of mRNA-LNPs by monocytes/macrophages after the addition of PS lipids that can bind to the PS receptors on these cells.[27] This observation echoes the in vitro transfection experiment where PS-LNP had a higher Fluc expression than MC3-LNP in RAW264.7 and primary mouse splenocytes. Furthermore, we discovered an increased number of the $Ly6C^{Hi}$ (classical/inflammatory) and the $Ly6C^{lo\text{-}neg}$ subset (nonclassical/anti-inflammatory) in mRNA-LNP treated groups compared to in the PBS control group. However, only PS-LNP treated group has much higher $Cy5^+$ cell populations than MC3-LNP (Figure S12). It implies that the incorporation of PS lipids could induce recruitment and activation of blood or tissue-derived monocytes, facilitating the uptake and targeting of PS-LNP to the secondary lymphoid tissue. The uptake of Cy5-RNA by other cell populations, including eosinophils ($CD11b^+Ly6G^-Ly6C^{lo\text{-}neg}SSC^{Lo}$), neutrophils ($CD11b^+Ly6G^+$), dendritic cells ($CD11c^+F4/80^-$), and lymphocytes ($CD3e^+$ and $CD19^+$) were demonstrated in Figure 4D.

To investigate the cellular uptake of LNPs in the lymph node, we imaged the tissue sections of SCLNs from mice administered with MC3- and PS-LNP using a confocal microscope, respectively (Figure 4E). $Cy5^+$ cells were more populated in PS-LNP than that in MC3-LNP. Most of them are located at the subcapsular sinus of the LN, where afferent macrophages bring antigenic information and relay it to B cells or T cells to activate adaptive immune responses.[30] Immunohistochemistry was performed on thin sections of SCLNs using anti-CD11b and anti-CD169 antibodies to identify the cell type of $Cy5^+$ cells.[31,32] In MC3-LNP, the Cy5 signal was distributed sparsely and dimly in the LN with a few in $CD11b^+$ cells. On the contrary, in PS-LNP, most of the mRNA ($Cy5^+$) was taken up by monocytes ($CD11b^+$) or subcapsular sinus macrophages ($CD11b^+CD169^+$) (Figure 4F). Therefore, the delivery of mRNA by PS-LNP is mediated by monocytes/macrophages.

To further corroborate the determining role of macrophages in the SLO-targeting capabilities of PS-LNP, we delivered the LNP and localized the protein expression in a macrophage-depleted mouse model. Briefly, C57BL/6J mice were intravenously treated with clodronate-liposomes (Clodrosome) at 18 h before the administration of mRNA-LNPs (Figure 5A).

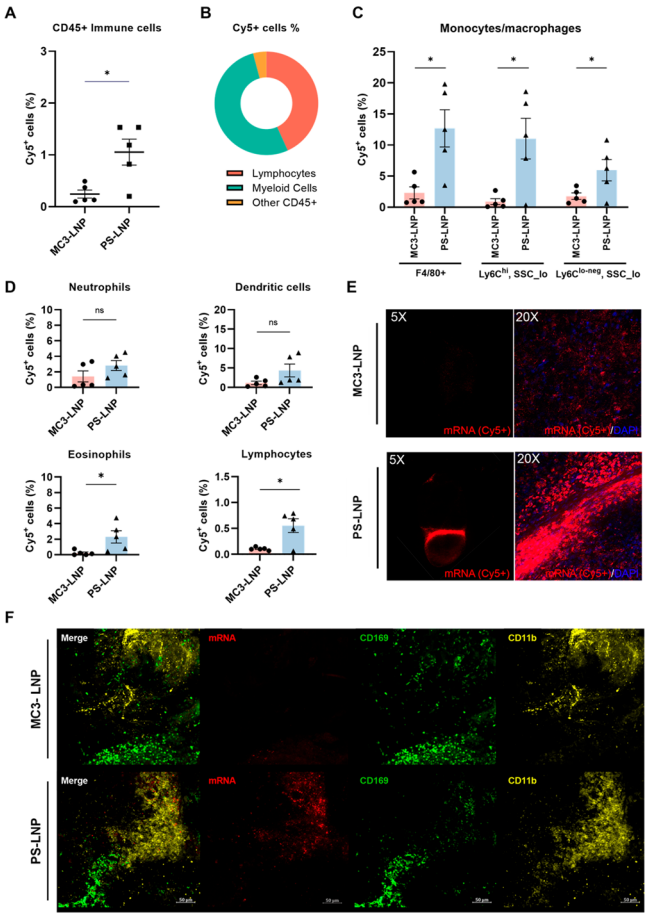

Figure 4. Analysis of the cell types that take up PS-LNP by flow cytometry and confocal microscopy. (A-D) Flow cytometry analysis of $Cy5^+$ cells extracted from spleens of mice treated with MC3-LNP and PS-LNP. (A) PS-LNP treated group has a higher percentage of $Cy5^+$ transfected cells in $CD45^+$ immune cells than MC3-LNP. (B) The breakdown of $CD45^+$ immune cells from the PS-LNP treated group. 52.6% of $Cy5^+$ cells are myeloid cells and 43.2% are lymphocytes. (C) Quantification of the percentage of $Cy5^+$ cells within monocyte/macrophage defined by F4/80-based ($CD11b^+F4/80^+$) and Ly6G/Ly6C-based ($CD11b^+Ly6G^-Ly6C^{Lo\text{-}neg}SSC^{Lo}$ and $CD11b^+Ly6G^-Ly6C^{Hi}SSC^{Lo}$) strategies, respectively. The percentage of monocytes/macrophages that take up PS-LNP was more than 2-fold higher than MC3-LNP. (D) Quantification of the percentage of Cy5+ cells within defined cell type populations, including neutrophils ($CD11b^+Ly6G^+$), eosinophils ($CD11b^+Ly6G^-Ly6C^{Lo\text{-}neg}SSC^{Hi}$), dendritic cells ($CD11c^+F4/80^-$) and lymphocytes ($CD19^+$ and $CD3e^+$) (E) Confocal images of a representative SCLN from a mouse treated with MC3- and PS-LNP encapsulating Cy5-RNA. It confirmed the potent uptake of PS-LNP, which was mostly located in the subcapsular sinus zone. (F) Immunohistochemical staining was performed on the thin SCLN section from mice treated with MC3- and PS-LNP, respectively. Markers are indicated as Cy5-RNA (Red), CD169 (Green), and CD11b (Yellow). While the Cy5 signal was barely seen in MC3-LNP, PS-LNP was shown to be taken up by subcapsular sinus macrophages ($CD11b^+CD169^+$). Data are shown as mean ± SEM ($n = 5$). A two-tailed unpaired student t test was used to analyze the statistical significance of between data indicated (** $p < 0.01$; *** $p < 0.001$; **** $p < 0.0001$). Data are shown as mean ± SEM.

Clodrosome is a well-characterized liposomal drug that is used to deplete macrophages either in peripheral blood or local tissues, depending on injection routes, in animals.[31,33,34] As shown in Figure 5B, PS-LNP no longer delivered mRNA to

https://doi.org/10.1021/acs.nanolett.2c03234
Nano Lett. 2022, 22, 8304−8311

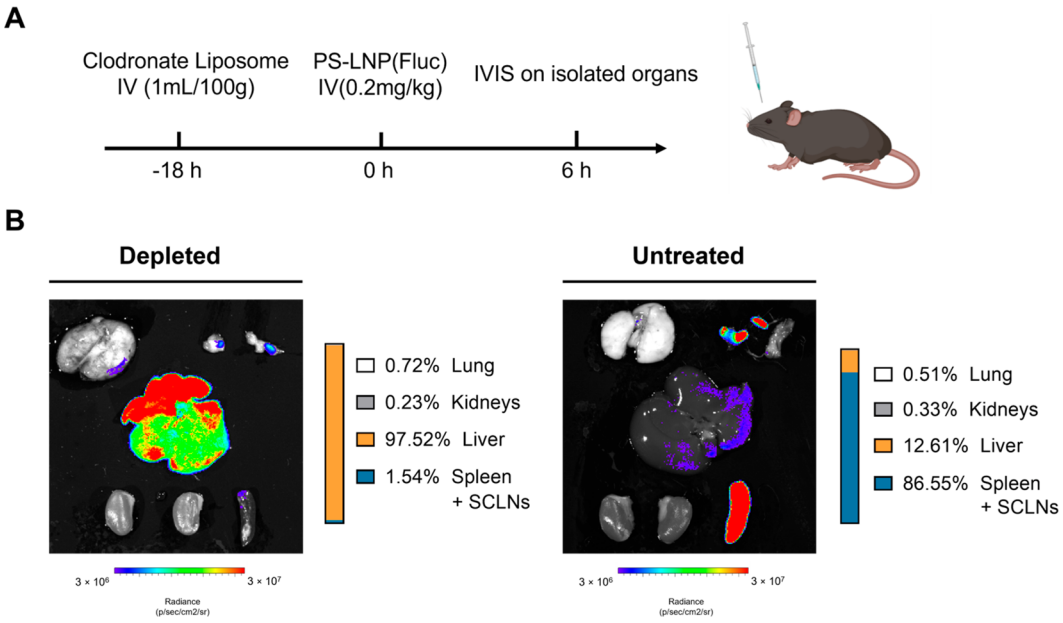

Figure 5. (A) Clodronate liposome was given to C57BL/6J to deplete macrophages. PS-LNP carrying Fluc-mRNA was administered (0.2 mg/kg) at 18-h after the treatment (figure was created with BioRender.com). (B) IVIS images were taken on isolated organs at 6 h after the injection of LNPs. The result clearly showed that most of the expression (>97%) occurred in the liver after macrophage depletion (left). Depletion of macrophages voids the targeted delivery of PS-LNP to SLOs, indicating the targeting effect is macrophage-mediated.

SLOs in Clodrosome-treated mice. Instead, Fluc expression predominantly occurred in the liver with more than 97% of expression among other major organs. Depletion of macrophages in the mouse completely switches the protein expression of PS-LNP back to the liver, suggesting a pivotal role of these immune cells in determining the SLOs targeting capabilities of PS-LNP.

To summarize, we reported a PS-containing LNP system, PS-LNP, for the systemic and targeted delivery of mRNA into SLOs. It should be pointed out that the "targeting" capacity of mRNA-LNPs in the literature could refer to a) high accumulation of mRNA-LNPs in the targeted organ, or b) high mRNA transfection efficiency characterized by protein expression from the targeted organ. For mRNA-LNPs, high accumulation in the targeted organ does not necessarily indicate successful and efficient cellular uptake and protein expression of the mRNA.[18,19,35] Hence, we compared the targeting effect among MC3-, PA-, and PS-LNP by studying both the organ-specific protein expression and particle accumulation. Our results showed that PS-LNP induced a stronger mRNA expression selectively in the spleen and SCLNs, although it had a similar particle biodistribution in the liver and the spleen as PA-LNP. We have demonstrated that SLOs targeting is not simply due to anionic lipids used. Instead, a biomimetic functional group, phosphoserine, facilitates the cell-mediated targeted delivery of LNPs rather than simply charge-dependent organ-specific accumulation. *In vitro* and *in vivo* characterizations of PS-LNP verified that its SLOs-targeting effect is mediated by monocytes/macrophages. While other studies utilized anionic lipids, including PS and PA, to tune the surface charge of LNPs,[18,25] this work has pointed out the role of a biomimetic PS in cell-particle interactions to achieve efficient targeted delivery. Overall, this work provides a new approach for the design of SLOs-targeting delivery.

■ ASSOCIATED CONTENT

Supporting Information

The Supporting Information is available free of charge at https://pubs.acs.org/doi/10.1021/acs.nanolett.2c03234.

All material and methods used in this work, the detailed formulation of LNPs, the Cyro-EM image of LNPs, IVIS images of all biological replicates, in vitro transfection assay, and gating strategies of flow analysis (PDF)

■ AUTHOR INFORMATION

Corresponding Author

Shaoyi Jiang − *Meinig School of Biomedical Engineering, Cornell University, Ithaca, New York 14853, United States;* orcid.org/0000-0001-9863-6899; Email: sj19@cornell.edu

Authors

Sijin Luozhong − *Meinig School of Biomedical Engineering, Cornell University, Ithaca, New York 14853, United States;* orcid.org/0000-0001-8697-9480

Zhefan Yuan − *Meinig School of Biomedical Engineering, Cornell University, Ithaca, New York 14853, United States;* orcid.org/0000-0002-4724-6214

Tara Sarmiento − *Meinig School of Biomedical Engineering, Cornell University, Ithaca, New York 14853, United States*

Yu Chen − *Department of Materials Science and Engineering, Cornell University, Ithaca, New York 14853, United States*

Wenchao Gu − *Meinig School of Biomedical Engineering, Cornell University, Ithaca, New York 14853, United States;* orcid.org/0000-0002-0967-1682

Caleb McCurdy − *Meinig School of Biomedical Engineering, Cornell University, Ithaca, New York 14853, United States*

Wenting Gao − *Department of Microbiology and Immunology, Cornell University, Ithaca, New York 14853, United States*

Ruoxin Li − *Meinig School of Biomedical Engineering, Cornell University, Ithaca, New York 14853, United States*

https://doi.org/10.1021/acs.nanolett.2c03234
Nano Lett. 2022, 22, 8304−8311

Stephan Wilkens − *Department of Biochemistry and Molecular Biology, SUNY Upstate Medical University, Syracuse, New York 13210, United States*

Complete contact information is available at: https://pubs.acs.org/10.1021/acs.nanolett.2c03234

Author Contributions

#S.L. and Z.Y. contributed equally.

Author Contributions

Conceptualization, S.L., Z.Y., S.J.; Methodology, S.L., Z.Y., S.J.; Investigation and experimentation, S.L., Z.Y., T.S., Y.C., W.G.U., C.M., W.GA., R.L., S.W.; Writing, S.L., Z.Y., S.J.

Notes

The authors declare the following competing financial interest(s): S.L., Z.Y., and S.J. are authors of a patent application related to this work (PCT/US21/64639) filed by Cornell University. All other authors declare that they have no competing interests.

■ ACKNOWLEDGMENTS

S.J. gratefully acknowledges financial support from the National Science Foundation (DMR 2002940) and start-up support from Cornell University, including Robert S. Langer Professorship and Cornell NEXT Nano Initiative. Imaging data were acquired through the Cornell Institute of Biotechnology's Imaging Facility, with NIH S10OD025049 for the IVIS Spectrum. S.W. is supported by NIH grant R35 GM141908. The Cryo-EM analysis was performed at the State University of New York College for Environmental Science and Forestry Analytical & Technical Services facility.

■ ABBREVIATIONS

PS, phosphatidylserine; LNP, lipid nanoparticle; SLO, secondary lymphoid organ;

■ REFERENCES

(1) Dolgin, E. The tangled history of mRNA vaccines. *Nature* **2021**, *597* (7876), 318−324.
(2) Cullis, P. R.; Hope, M. J. Lipid Nanoparticle Systems for Enabling Gene Therapies. *Mol. Ther* **2017**, *25* (7), 1467−1475.
(3) Hajj, K. A.; Whitehead, K. A. Tools for translation: non-viral materials for therapeutic mRNA delivery. *Nature Reviews Materials* **2017**, *2* (10), 17056.
(4) Jayaraman, M.; Ansell, S. M.; Mui, B. L.; Tam, Y. K.; Chen, J.; Du, X.; Butler, D.; Eltepu, L.; Matsuda, S.; Narayanannair, J. K.; Rajeev, K. G.; Hafez, I. M.; Akinc, A.; Maier, M. A.; Tracy, M. A.; Cullis, P. R.; Madden, T. D.; Manoharan, M.; Hope, M. J. Maximizing the potency of siRNA lipid nanoparticles for hepatic gene silencing in vivo. *Angew. Chem., Int. Ed. Engl.* **2012**, *51* (34), 8529−33.
(5) Pardi, N.; Tuyishime, S.; Muramatsu, H.; Kariko, K.; Mui, B. L.; Tam, Y. K.; Madden, T. D.; Hope, M. J.; Weissman, D. Expression kinetics of nucleoside-modified mRNA delivered in lipid nanoparticles to mice by various routes. *J. Controlled Release* **2015**, *217*, 345−51.
(6) Kauffman, K. J.; Dorkin, J. R.; Yang, J. H.; Heartlein, M. W.; DeRosa, F.; Mir, F. F.; Fenton, O. S.; Anderson, D. G. Optimization of Lipid Nanoparticle Formulations for mRNA Delivery in Vivo with Fractional Factorial and Definitive Screening Designs. *Nano Lett.* **2015**, *15* (11), 7300−6.
(7) Miao, L.; Lin, J.; Huang, Y.; Li, L.; Delcassian, D.; Ge, Y.; Shi, Y.; Anderson, D. G. Synergistic lipid compositions for albumin receptor mediated delivery of mRNA to the liver. *Nat. Commun.* **2020**, *11* (1), 2424.
(8) Sabnis, S.; Kumarasinghe, E. S.; Salerno, T.; Mihai, C.; Ketova, T.; Senn, J. J.; Lynn, A.; Bulychev, A.; McFadyen, I.; Chan, J.; Almarsson, O.; Stanton, M. G.; Benenato, K. E. A Novel Amino Lipid Series for mRNA Delivery: Improved Endosomal Escape and Sustained Pharmacology and Safety in Non-human Primates. *Mol. Ther* **2018**, *26* (6), 1509−1519.
(9) Kulkarni, J. A.; Cullis, P. R.; van der Meel, R. Lipid Nanoparticles Enabling Gene Therapies: From Concepts to Clinical Utility. *Nucleic Acid Ther* **2018**, *28* (3), 146−157.
(10) Tsoi, K. M.; MacParland, S. A.; Ma, X. Z.; Spetzler, V. N.; Echeverri, J.; Ouyang, B.; Fadel, S. M.; Sykes, E. A.; Goldaracena, N.; Kaths, J. M.; Conneely, J. B.; Alman, B. A.; Selzner, M.; Ostrowski, M. A.; Adeyi, O. A.; Zilman, A.; McGilvray, I. D.; Chan, W. C. Mechanism of hard-nanomaterial clearance by the liver. *Nat. Mater.* **2016**, *15* (11), 1212−1221.
(11) Hou, X.; Zaks, T.; Langer, R.; Dong, Y. Lipid nanoparticles for mRNA delivery. *Nat. Rev. Mater.* **2021**, 1−17.
(12) Schudel, A.; Francis, D. M.; Thomas, S. N. Material design for lymph node drug delivery. *Nat. Rev. Mater.* **2019**, *4* (6), 415−428.
(13) Liang, F.; Lindgren, G.; Lin, A.; Thompson, E. A.; Ols, S.; Rohss, J.; John, S.; Hassett, K.; Yuzhakov, O.; Bahl, K.; Brito, L. A.; Salter, H.; Ciaramella, G.; Lore, K. Efficient Targeting and Activation of Antigen-Presenting Cells In Vivo after Modified mRNA Vaccine Administration in Rhesus Macaques. *Mol. Ther* **2017**, *25* (12), 2635−2647.
(14) Loughrey, D.; Dahlman, J. E. Non-liver mRNA Delivery. *Acc. Chem. Res.* **2022**, *55* (1), 13−23.
(15) Veiga, N.; Goldsmith, M.; Granot, Y.; Rosenblum, D.; Dammes, N.; Kedmi, R.; Ramishetti, S.; Peer, D. Cell specific delivery of modified mRNA expressing therapeutic proteins to leukocytes. *Nat. Commun.* **2018**, *9* (1), 4493.
(16) Mitchell, M. J.; Billingsley, M. M.; Haley, R. M.; Wechsler, M. E.; Peppas, N. A.; Langer, R. Engineering precision nanoparticles for drug delivery. *Nat. Rev. Drug Discov* **2021**, *20* (2), 101−124.
(17) Kranz, L. M.; Diken, M.; Haas, H.; Kreiter, S.; Loquai, C.; Reuter, K. C.; Meng, M.; Fritz, D.; Vascotto, F.; Hefesha, H.; Grunwitz, C.; Vormehr, M.; Husemann, Y.; Selmi, A.; Kuhn, A. N.; Buck, J.; Derhovanessian, E.; Rae, R.; Attig, S.; Diekmann, J.; Jabulowsky, R. A.; Heesch, S.; Hassel, J.; Langguth, P.; Grabbe, S.; Huber, C.; Tureci, O.; Sahin, U. Systemic RNA delivery to dendritic cells exploits antiviral defence for cancer immunotherapy. *Nature* **2016**, *534* (7607), 396−401.
(18) Cheng, Q.; Wei, T.; Farbiak, L.; Johnson, L. T.; Dilliard, S. A.; Siegwart, D. J. Selective organ targeting (SORT) nanoparticles for tissue-specific mRNA delivery and CRISPR-Cas gene editing. *Nat. Nanotechnol* **2020**, *15* (4), 313−320.
(19) Dilliard, S. A.; Cheng, Q.; Siegwart, D. J. On the mechanism of tissue-specific mRNA delivery by selective organ targeting nanoparticles. *Proc. Natl. Acad. Sci. U. S. A.* **2021**, *118* (52), No. e2109256118.
(20) Segawa, K.; Nagata, S. An Apoptotic 'Eat Me' Signal: Phosphatidylserine Exposure. *Trends Cell Biol.* **2015**, *25* (11), 639−650.
(21) Amara, A.; Mercer, J. Viral apoptotic mimicry. *Nat. Rev. Microbiol* **2015**, *13* (8), 461−9.
(22) Kowalski, P. S.; Rudra, A.; Miao, L.; Anderson, D. G. Delivering the Messenger: Advances in Technologies for Therapeutic mRNA Delivery. *Mol. Ther* **2019**, *27* (4), 710−728.
(23) Fenton, O. S.; Kauffman, K. J.; Kaczmarek, J. C.; McClellan, R. L.; Jhunjhunwala, S.; Tibbitt, M. W.; Zeng, M. D.; Appel, E. A.; Dorkin, J. R.; Mir, F. F.; Yang, J. H.; Oberli, M. A.; Heartlein, M. W.; DeRosa, F.; Langer, R.; Anderson, D. G. Synthesis and Biological Evaluation of Ionizable Lipid Materials for the In Vivo Delivery of Messenger RNA to B Lymphocytes. *Adv. Mater.* **2017**, *29* (33), 1606944.
(24) Shi, B.; Keough, E.; Matter, A.; Leander, K.; Young, S.; Carlini, E.; Sachs, A. B.; Tao, W.; Abrams, M.; Howell, B.; Sepp-Lorenzino, L. Biodistribution of small interfering RNA at the organ and cellular levels after lipid nanoparticle-mediated delivery. *J. Histochem Cytochem* **2011**, *59* (8), 727−40.

(25) LoPresti, S. T.; Arral, M. L.; Chaudhary, N.; Whitehead, K. A. The replacement of helper lipids with charged alternatives in lipid nanoparticles facilitates targeted mRNA delivery to the spleen and lungs. *J. Controlled Release* **2022**, *345*, 819−831.
(26) Birge, R. B.; Boeltz, S.; Kumar, S.; Carlson, J.; Wanderley, J.; Calianese, D.; Barcinski, M.; Brekken, R. A.; Huang, X.; Hutchins, J. T.; Freimark, B.; Empig, C.; Mercer, J.; Schroit, A. J.; Schett, G.; Herrmann, M. Phosphatidylserine is a global immunosuppressive signal in efferocytosis, infectious disease, and cancer. *Cell Death Differ.* **2016**, *23* (6), 962−78.
(27) Naeini, M. B.; Bianconi, V.; Pirro, M.; Sahebkar, A. The role of phosphatidylserine recognition receptors in multiple biological functions. *Cell Mol. Biol. Lett.* **2020**, *25*, 23.
(28) Rose, S.; Misharin, A.; Perlman, H. A novel Ly6C/Ly6G-based strategy to analyze the mouse splenic myeloid compartment. *Cytometry A* **2012**, *81A* (4), 343−50.
(29) Liu, Z.; Gu, Y.; Shin, A.; Zhang, S.; Ginhoux, F. Analysis of Myeloid Cells in Mouse Tissues with Flow Cytometry. *STAR Protoc* **2020**, *1* (1), 100029.
(30) Gray, E. E.; Cyster, J. G. Lymph node macrophages. *J. Innate Immun* **2012**, *4* (5−6), 424−36.
(31) Tacconi, C.; Commerford, C. D.; Dieterich, L. C.; Schwager, S.; He, Y.; Ikenberg, K.; Friebel, E.; Becher, B.; Tugues, S.; Detmar, M. CD169(+) lymph node macrophages have protective functions in mouse breast cancer metastasis. *Cell Rep* **2021**, *35* (2), 108993.
(32) Louie, D. A. P.; Liao, S. Lymph Node Subcapsular Sinus Macrophages as the Frontline of Lymphatic Immune Defense. *Front Immunol* **2019**, *10*, 347.
(33) van Rooijen, N.; van Kesteren-Hendrikx, E. Clodronate liposomes: perspectives in research and therapeutics. *J. Liposome Res.* **2002**, *12* (1−2), 81−94.
(34) van Rooijen, N.; Hendrikx, E. Liposomes for specific depletion of macrophages from organs and tissues. *Methods Mol. Biol.* **2010**, *605*, 189−203.
(35) Qiu, M.; Tang, Y.; Chen, J.; Muriph, R.; Ye, Z.; Huang, C.; Evans, J.; Henske, E. P.; Xu, Q. Lung-selective mRNA delivery of synthetic lipid nanoparticles for the treatment of pulmonary lymphangioleiomyomatosis. *Proc. Natl. Acad. Sci. U. S. A.* **2022**, *119* (8), No. e2116271119.

https://doi.org/10.1021/acs.nanolett.2c03234
Nano Lett. 2022, 22, 8304−8311